

# Reverse-Flow Operation for Application of Imperfectly Immobilized Catalysts

Kim G. W. Hung, Dennis Papadias, and Pehr Björnbom

Royal Institute of Technology (KTH), Dept. of Chemical Engineering and Technology,  
Division of Chemical Reaction Engineering, SE-100 44, Stockholm, Sweden

Magnus Anderlund and Björn Åkermark

Stockholm University, Arrhenius Laboratory, SE-106 91, Stockholm, Sweden

*A reverse-flow packed-bed reactor used to solve the problem of leaching from immobilized homogeneous catalysts was studied. Product-to-catalyst ratios (PCRs) for a reverse-flow reactor (RFR) and a conventional batch reactor with catalyst reuse were compared theoretically and numerically. In the ideal case without band broadening in the RFR it is possible to completely eliminate the limit on PCR due to leaching, but in practice, band broadening, caused by kinetic and dispersion effects, cannot be avoided. Nonetheless, numerical experiments showed numerous cases with much higher PCRs for the RFR than for batch operation with catalyst reuse. Therefore, an RFR may be a successful solution in cases when catalyst leaching is too high for using batch operation with catalyst reuse. The design and operation of a suitable RFR are also discussed.*

## Introduction

Today, the batch reactor is generally used for homogeneously catalyzed reactions. A central problem is the recovery of the catalyst.

A solution to that problem is biphasic catalysis. A successful example is the Rhône-Poulenc/Ruhr-Chemie Process for the hydroformylation of olefins (Cornils and Kuntz, 1995), where the catalyst complex is made water soluble, which permits its separation from the organic phase containing the reactant and the product after the reaction.

One form of biphasic catalysis is immobilization of the catalyst by bonding to a solid support. Very strong, often covalent, bonds between catalyst and support characterize a successful catalyst immobilization, for example, the well-known TS-1 (Sheldon et al., 1998). These strong bonds give no or very little catalyst solubility in the liquid phase. However, preparation of the strongly bonded supported catalysts is often complicated and has not been possible to achieve for many interesting homogeneous metal organic catalysts. A common problem is the leaching of catalyst from the solid support due to excessive solubility in the liquid phase. Moreover, if the catalyst is strongly bonded to the solid support, the result is

often a less active catalyst, although the opposite effect may also occur (Wöltinger et al., 1999).

Another solution to the catalyst immobilization problem would be to decrease the requirements of very strong bonds and extremely low catalyst solubility. If weaker bonds would be sufficient, the preparation of an immobilized catalyst would be easier, and more common sorption agents and methods could be used. In the present article, we discuss the possibility of using reverse-flow operation in order to use such imperfectly immobilized catalysts in a packed-bed reactor. In this case, the catalyst will migrate within the reactor as in chromatography. By reversal of the flow, the catalyst is prevented from leaving the bed when it has reached an end of the reactor. In this way, the catalyst is trapped within the reactor in order to be better utilized. The principle of the reverse-flow reactor (RFR) is shown in Figure 1.

An example of possible applications of this reactor concept could be imperfectly immobilized homogeneous catalysts for fine chemical production. In favorable cases, reverse-flow operation could turn a leaking catalyst immobilization into a successful process solution.

This work was partly presented previously in two AIChE Annual Meeting papers (Hung et al., 2000; Björnbom et al., 2001).

Correspondence concerning this article should be addressed to P. Björnbom.

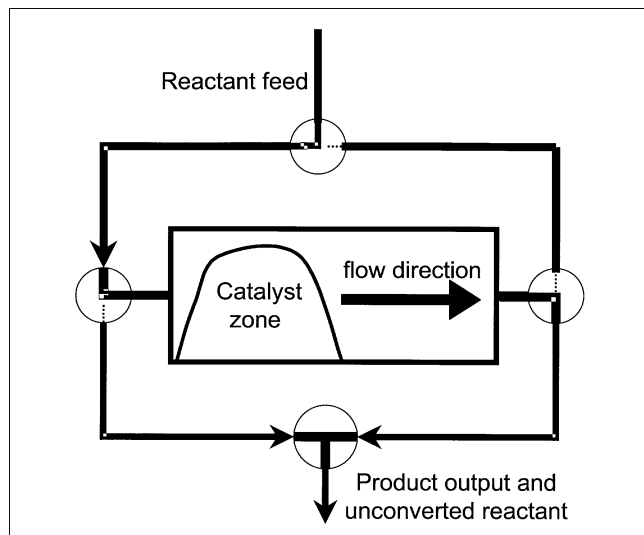


**Figure 1. Principle of the RFR with partially immobilized catalyst.**

### Short history of the reverse-flow reactor

As early as 1938, Cottrell patented the concept of the RFR. Compared to the conventional steady-state reactors, the advantages of the RFR are, for example, better yields, lower reactor exit temperature, and less need of preheaters. Until now, the RFR concept has mainly found the following applications:

- SO<sub>2</sub> oxidation (Boreskov et al., 1979; Boreskov and Matros, 1983)
- Removal of nitrogen oxides (Bobrova et al., 1988)
- Production of syngas (Blanks et al., 1990)
- Methanol synthesis (Neophytides and Froment, 1992)
- Catalytic combustion of VOC (Nieken et al., 1994; van de Beld, 1995)
- Catalytic oxidation of CO (Züfle and Turek, 1997)

Matros and Bunimovich (1996) presented a comprehensive review of these applications.

Neophytides and Tripakis (1996) applied the RFR concept on a solid oxide fuel cell (SOFC) monolith. More recently, Matros et al. (1999) investigated applications of the concept for automotive emission control.

Evaluation of the dynamic features of the RFR using the bifurcation analysis is extensively used, for example, by Khinast et al. (1999).

The main purpose of the reverse operation cited earlier was to keep an elevated temperature profile within the reactor. Agar and Ruppel (1988) transferred the RFR concept from energy trapping to mass trapping. Here, a zone of adsorbed ammonia is kept within the reactor to react with nitric oxide under selective catalytic reduction of NO<sub>x</sub>. As an extension, simulation results by Snyder and Subramanian (1998) showed that RFR with side-stream feed is an attractive process for maximum utilization of reactive species that adsorb on catalysts.

Kallrath et al. (1993) have made a more general numerical study of an RFR in which gaseous reactants are adsorbed onto a solid catalyst. Falle et al. (1995) showed that an RFR with feed of the adsorbing species in the midsection could be

more efficient than a conventional reactor. Also, they concluded that the performance is largely determined by the adsorption and desorption processes.

So far, the treatment of reverse-flow operation in the literature has mainly dealt with heat trapping and reactant-mass trapping. Our present work, which may be referred to as catalyst-mass trapping, concerns another type of application of reverse-flow operation. To our knowledge the only similar work, besides our own (Hung et al., 2000; Björnbom and Åkermark, 2001; Björnbom et al., 2001), is the discussion of reverse flow operation of a packed bed for an alkylation process in a patent application by Hommeltoft and Topsøe (1991).

### Objectives

The objective of this work has been to carry out a theoretical and numerical study of the performance of the RFR compared to conventional reactors such as the batch reactor and the completely immobilized catalytic single-pass packed-bed reactor. Simple catalytic model reactions have been assumed and a mathematical model has been formulated for simulation of the RFR. The possibilities and limitations of the concept will be discussed.

### Formulation of the Model

Let the mechanism of the model reaction be



Here, we consider a one-dimensional isothermal packed-bed reactor in which flows a reactant (*A*), reacting with both (*B*) and (*C*), where *B* is the catalyst in the fluid phase, and *C* is the catalyst sorbed in the solid support. We assume that the product, *D*, is formed irreversibly by the reaction. The reaction mechanisms in the fluid phase and on the solid support are illustrated in Figure 2. Analogy can be made with chromatographic systems.

First, *B* is introduced into the upstream part of the reactor as a band or region. Initially, dynamical equilibrium between *B* and *C* is assumed to be established. If the adsorption and desorption rates are large and the solid support has a large sorption capacity and/or the catalyst has a high affinity, then the band of catalyst that moves slowly downstream compared to the fluid flow will have sharp boundaries. The purpose of the flow-reversal mode is to prevent *B* and *C* from leaving the reactor.

In order to simplify the reactor model, we have made the following assumptions (if nothing else is mentioned):

- The fluid is incompressible.
- Catalytic species *B* and *C* act as single sites for the reaction.
- The reactant and the product are not sorbed at all on the solid support. Only the catalyst is partially sorbed.
- The same dispersion coefficient for all species.
- Equation 1 is irreversible first-order with respect to both *A* and *B*.

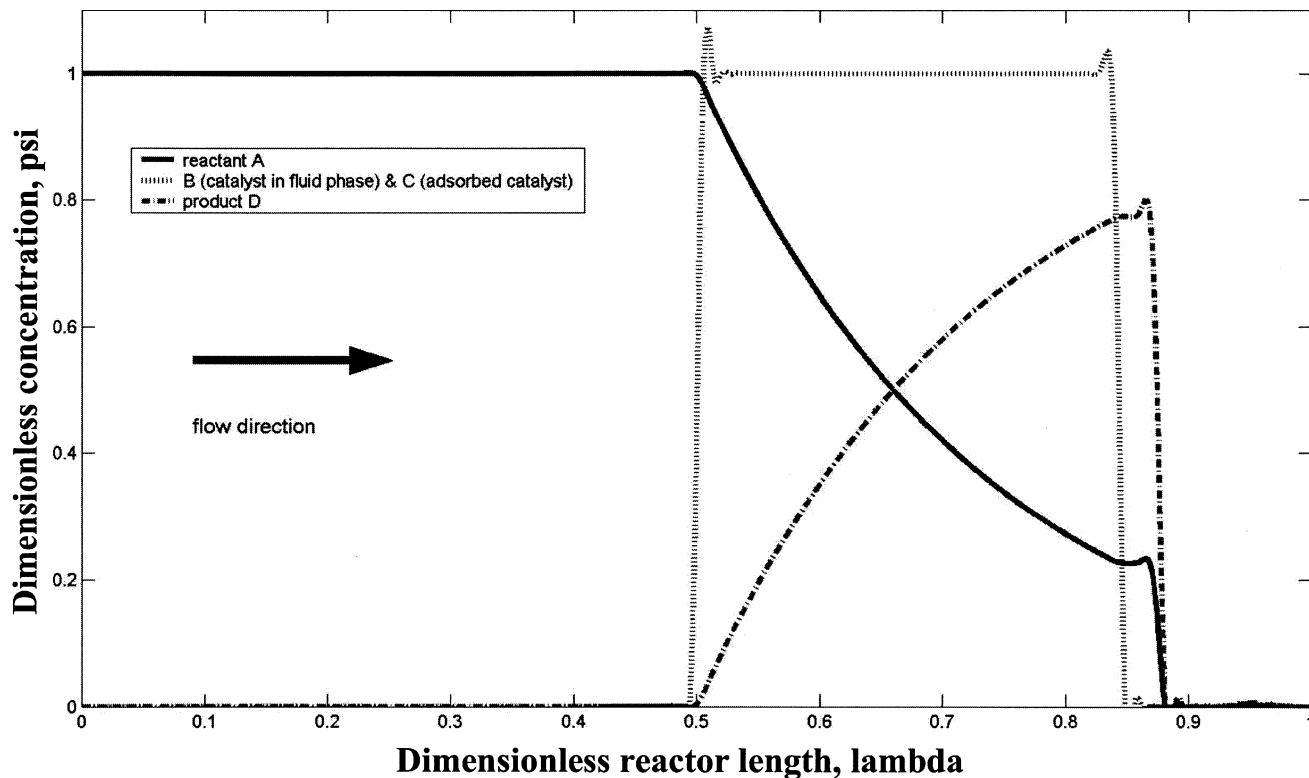


**Figure 2. Concentration profile in an ideal RFR at time  $\theta = 0.35$ .**

Parameters:  $K = 0.5$ ,  $L = 4.5$  m,  $C_{K0} = 0.01$ ,  $\delta = 0.34$ ,  $Pe = \text{inf}$ ,  $Da_2 = \text{inf}$ . The solid line represents the reactant concentration profile, the dashed line the catalyst in the fluid and the solid support, and the dash dotted line the product.

- Equation 2 is irreversible first-order with respect to both  $A$  and  $C$ .

- Equation 3 is reversible and of the first order.

- All rate equations involving the support phase are assumed to give apparent rates, including both external and internal mass-transfer resistances.

- The average concentration of  $C$  in the support on a volume basis is used.

- The sorption isotherm for the catalyst has a simple form, equivalent to Henry's law.

- The catalyst is equally active in both the fluid phase and on the solid support.

- The catalyst deactivation is neglected in this study.

- The reactor is considered to be isothermal.

With the preceding formulation, mass balances using the dispersion model for the packed-bed reactor result in the following PDE system in dimensionless form (Eqs. 4–7), which then is solved by FEMLAB (Femlab, 1999), a numerical solver using the finite-element method. Comparisons between the Femlab solutions and solutions according to the method of lines showed good agreement.

$$\frac{1}{Pe} \frac{\partial^2 \Psi_A}{\partial \lambda^2} - \frac{\partial \Psi_A}{\partial \lambda} - Da_1 (\epsilon \Psi_B + (1 - \epsilon) K \Psi_C) \Psi_A = \epsilon \frac{\partial \Psi_A}{\partial \theta} \quad (4)$$

$$\frac{1}{Pe} \frac{\partial^2 \Psi_B}{\partial \lambda^2} - \frac{\partial \Psi_B}{\partial \lambda} + Da_2 (\Psi_C - \Psi_B) = \epsilon \frac{\partial \Psi_B}{\partial \theta} \quad (5)$$

$$Da_2 \frac{1}{K} (\Psi_B - \Psi_C) = (1 - \epsilon) \frac{\partial \Psi_C}{\partial \theta} \quad (6)$$

$$\frac{1}{Pe} \frac{\partial^2 \Psi_D}{\partial \lambda^2} - \frac{\partial \Psi_D}{\partial \lambda} + Da_1 (\epsilon \Psi_B + (1 - \epsilon) K \Psi_C) \Psi_A = \epsilon \frac{\partial \Psi_D}{\partial \theta}, \quad (7)$$

where  $\Psi$  and  $\theta$  are defined as the dimensionless concentrations and time:

$$\Psi_A = \frac{C_A}{C_{A0}}, \quad \Psi_B = \frac{C_B}{C_{B0}}, \quad \Psi_C = \frac{C_C}{C_{C0}},$$

$$\Psi_D = \frac{C_D}{C_{A0}}, \quad \theta = \frac{tU}{L}.$$

The following dimensionless parameters are defined as

$$Pe = \frac{UL}{D_e}, \quad Da_1 = \frac{k_1 C_{B0} L}{U}, \quad Da_2 = \frac{k_2 La}{U}.$$

The following condition is assumed:

$$\frac{C_{C0}}{C_{B0}} = K.$$

### Initial conditions

$$A: \Psi_A = 0, \quad 0 < \lambda < 1$$

$$B: \Psi_B = 1, \quad 0 < \lambda < \delta$$

$$\Psi_B = 0, \quad \delta < \lambda < 1$$

$$C: \Psi_C = 1, \quad 0 < \lambda < \delta$$

$$\Psi_C = 0, \quad \delta < \lambda < 1$$

$$D: \Psi_D = 0, \quad 0 < \lambda < 1.$$

### Boundary conditions

Two sets of boundary conditions were used. The Danckwerts boundary conditions were always used for the reactant and the product. However, for *B*, the dissolved catalyst, we studied two kinds of boundary conditions. This boundary condition for *B* may significantly influence the calculation results. Therefore we tried two extremes of boundary conditions, case 1 and case 2. In case 2 Danckwerts' boundary conditions were also used for *B*.

*Case 1.* For flow toward the right end of the reactor:

$$\begin{aligned} \text{At } \lambda = 0 \text{ (left end of reactor): } \quad & \frac{\partial \Psi_A}{\partial \lambda} = 1 - \Psi_A; \quad \Psi_B = 0; \\ & \frac{\partial \Psi_D}{\partial \lambda} = -\Psi_D. \end{aligned}$$

$$\text{At } \lambda = 1 \text{ (right end of reactor): } \quad \frac{\partial \Psi_A}{\partial \lambda} = 0; \quad \Psi_B = 0; \quad \frac{\partial \Psi_D}{\partial \lambda} = 0.$$

*Case 2.* For flow toward the right end of the reactor:

$$\begin{aligned} \text{At } \lambda = 0 \text{ (left end of reactor): } \quad & \frac{\partial \Psi_A}{\partial \lambda} = 1 - \Psi_A; \\ & \frac{\partial \Psi_B}{\partial \lambda} = -\Psi_B; \quad \frac{\partial \Psi_D}{\partial \lambda} = -\Psi_D. \end{aligned}$$

$$\begin{aligned} \text{At } \lambda = 1 \text{ (right end of reactor): } \quad & \frac{\partial \Psi_A}{\partial \lambda} = 0; \quad \frac{\partial \Psi_B}{\partial \lambda} = 0; \\ & \frac{\partial \Psi_D}{\partial \lambda} = 0. \end{aligned}$$

For flow toward the left end of the reactor, the boundary conditions are reversed. The two cases are extremes in that the dissolved catalyst cannot pass the boundary by convection, but only by diffusion in case 1, while it is the other way around in case 2.

### An ideal case

By further assumptions it is possible to considerably simplify the mathematical treatment, bearing in mind that those assumptions may be far from reality in many cases and that

the model should be applied with much caution. The further assumptions are:

- Ideal plug flow in the reactor—that is, infinite Peclet number.
- No kinetic resistance for the sorption/desorption of the catalyst—that is, the Damköhler number for this reaction is infinite and the catalyst concentrations in the two phases satisfy the equilibrium condition.

This results in the following simplified mathematical model:

$$\Psi_B = \Psi_C \quad (8)$$

$$-\frac{\partial \Psi_A}{\partial \lambda} - Da_1 [\epsilon \Psi_B + (1 - \epsilon) K \Psi_B] \Psi_A = \epsilon \frac{\partial \Psi_A}{\partial \theta} \quad (9)$$

$$-\frac{\partial \Psi_B}{\partial \lambda} = [\epsilon + K(1 - \epsilon)] \frac{\partial \Psi_B}{\partial \theta} \quad (10)$$

$$-\frac{\partial \Psi_D}{\partial \lambda} + Da_1 (\epsilon \Psi_B + (1 - \epsilon) K \Psi_B) \Psi_A = \epsilon \frac{\partial \Psi_D}{\partial \theta} \quad (11)$$

$$Da_1 = \frac{k_1 C_{K0} L}{U}.$$

Equation 10 is derived by combining Eqs. 5, 6 and 8.

Let us consider the movement of a catalyst zone through the reactor. Since we have an ideal plug flow, the catalyst zone will move without changing its shape. Due to the sorption/desorption equilibrium, the catalyst zone will move with a lower velocity through the packed bed than the reactant solution. If the reactant solution has the velocity  $U_A = U/\epsilon$ , the catalyst zone will move with the velocity

$$U_B = U_C = \frac{U_A}{1 + K \frac{1 - \epsilon}{\epsilon}}. \quad (12)$$

We can easily derive Eq. 12 by applying Eq. 10 or a simple mass-balance argument.

The reactant will react when passing the slower-moving catalyst zone. If the bed is long enough, a quasi-steady-state will be established and the time derivative in Eq. 9 can be neglected. If we consider a catalyst zone with a constant catalyst concentration such that  $\Psi_B = \Psi_C = 1$ , we obtain the following analytical solution for the conversion over this zone:

$$X = 1 - \exp \left( - \frac{k_1 \delta L C_{K0}}{U_A - U_B} \right). \quad (13)$$

In the case of infinite  $K$ , that is, a perfectly immobilized catalyst, the catalyst zone will not migrate and Eq. 13 is reduced to the conversion for an ideal plug-flow reactor (PFR):

$$X = 1 - \exp \left( - \frac{k_1 L C_{K0}}{U_A} \right).$$

The process parameters assumed in this study are presented in Table 1.

**Table 1. Assumed Process Parameters**

Superficial velocity, $U$	0.001 m/s
Bed porosity, $\epsilon$	0.40
Specific reaction rate, $k_1$	0.04 m <sup>3</sup> /mol, s*
Initial catalyst concentration in the catalyst zone for the RFR or total catalyst concentration	1% of $C_{A0}$
for the batch reactor, $C_{K0}$	
Reactor length (PFR), $L$	3.6 m
Reactor length (RFR), $L$	4.5 m

\*This is the reaction rate corresponding to batch reactor data (conversion 81%, catalyst concentration 0.011 mol/L, residence time 1 h) taken from a tabular survey of reactions by Heck (1982). Note that we have used an artificial catalyst concentration of 1% in order to facilitate PCR calculations. Modifying the value of the specific reaction rate in such a way that the reaction rate is not changed has equalized this change in catalyst concentration.

### Criterion of separation

Moreover, the following criterion for separation of the product from the catalyst can be deduced for the minimum reactor length:

$$L > U_A \frac{\delta L}{U_A - U_B}, \quad (15)$$

giving a maximum length of catalyst zone for the ideal cases by using Eq. 12:

$$\delta < 1 - \frac{1}{1 + \frac{K}{\epsilon}(1 - \epsilon)}. \quad (16)$$

Only when the catalyst zone is narrower than  $\delta L$ , can product flow out of the reactor between the flow reversals. The smaller  $\delta$  is, the more products can be produced per cycle and the longer the cycle times will be.

In this study, the RFR length (4.5 m) has been assumed to be 20% longer compared to the single-pass reactor (3.6 m). This assumption has two purposes. The first is to ensure the separation of the product from the catalyst. Second, extra reactor space will be needed for the later cases, with band broadening of the catalyst zone.

Moreover, we have made the following assumptions for the process:

- Criteria for flow reversal: the catalyst concentration at the reactor end exceeds 1% of the initial concentration for the boundary conditions according to case 2. An estimation shows that the catalyst leakage in such a case is less than 0.5% per h for  $K$  values equal to or greater than 10. For the boundary conditions of case 1, the flow-reversal criterion was applied to the last grid point at 4.5 mm before the reactor outlet.

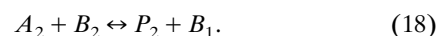
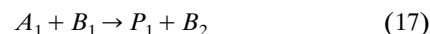
- The dead volumes outside the reactor, consisting of the two switch valves next to the reactor ends, and the tubing between the valves and the reactor ends and the catalyst trapping devices, are neglected.

### More complicated catalyst cycles

In the present study the numerical simulations have been limited to the model just presented with a simple isomerization reaction on a single-site catalyst. Here, we will discuss a

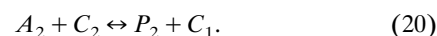
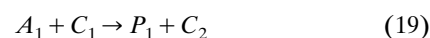
further example, but only for the ideal case without band broadening due to dispersion and kinetic resistance for the sorption/desorption reaction.

In redox reactions the catalyst alternates between an oxidized and a reduced form:



Here  $A_1$  may be an organic compound that is oxidized to  $P_1$  by the oxidized form of the homogeneous catalyst,  $B_1$ . In the second reaction, the oxidant,  $A_2$ , for example, hydrogen peroxide, is oxidizing the reduced form of the catalyst,  $B_2$ , forming a byproduct, for example, water. In this example, we assume that the first reaction is rate determining.

The corresponding reactions for the sorbed form of the catalyst are



The sorption/desorption reactions are assumed to be so fast that equilibrium is closely approached:



The equilibrium assumptions, together with the assumption of no dispersion, that is, ideal plug flow, give us an ideal case where the concentrations of the catalyst complexes are fully determined by the equilibrium conditions. Therefore, the migration velocity of the catalyst zone can be easily derived by the same methods that were used for Eq. 12. Since the equilibrium according to Eqs. 18 and 20 involve the oxidant and the byproduct, their concentrations will appear in the expression for this velocity:

$$U_K = \frac{U_A}{K_{21} + \frac{K_{22}C_{P2}}{K_{18}C_{A2}} \frac{1 - \epsilon}{1 + \frac{C_{P2}}{K_{18}C_{A2}} \frac{1 - \epsilon}{\epsilon}}} \quad (23)$$

Note that we get perfect immobilization if either  $K_{22}$  or  $K_{21}$  approaches infinity, that is, only one of the complexes must be strongly bound to the solid support to obtain this result. This is because the main part of the catalyst will be in the form of the strongly sorbed complex, while all other complexes will appear in trace concentrations. Note the obvious relation between low leakage and slow migration in a packed bed.

On the other hand, if Eqs. 18 and 20 were slow reactions, the oxidized and the reduced catalyst complexes would migrate decoupled, in general, at different velocities. In this case, both complexes  $C_1$  and  $C_2$  must be strongly bound to the solid support in order to get good immobilization. This case could lead to the formation of end zones of the catalyst

zone with only reduced or oxidized catalyst complexes. The catalytic reaction would stop in such zones. However, at flow reversal such a zone that was being formed would begin to disappear again.

Finally we can note an obvious case where reverse-flow operation would not help at all. This is the case where the leakage of catalyst from the solid support is an irreversible process. Then the dissolved catalyst will go straight out with the outlet flow without any retardation.

### Definition of PCR

To evaluate the performance of the reactors, a product catalyst ratio (PCR) was used. Higher PCR means higher efficiency of the catalyst usage. The PCR for the conventional batch and single-pass packed-bed reactors is defined simply by:

$$\text{PCR} = \frac{N_{\text{prod}}}{N_{\text{cat}}}$$

Because of the alternating behavior of the RFR, the PCR for the RFR is defined as the output amount of product divided by the amount of catalyst used in the RFR. The product left in the reactor is neglected since it is not separated from the catalyst. The amount of output product produced between two time-steps,

$$\Delta N_{\text{prod}} = \nu C_{A0} \tilde{\Psi}_D \Delta t,$$

where  $\Delta t$  is time step, and  $\nu = UA_c$  is the volumetric flow rate of fluid phase.

The output amount of product produced at a given point in time is determined by integration of the average product concentration,  $C_{A0} \tilde{\Psi}_D$ , at the output end of the reactor for all time steps:

$$\begin{aligned} N_{\text{prod}} &= \sum \Delta N_{\text{prod}} = \nu C_{A0} \sum \tilde{\Psi}_D \Delta t = UA_c C_{A0} \sum \tilde{\Psi}_D \Delta t \\ &= UA_c C_{A0} \sum \tilde{\Psi}_D \frac{\Delta \theta L}{U} = C_{A0} LA_c \sum \tilde{\Psi}_D \Delta \theta. \end{aligned}$$

The amount of catalyst initially loaded is

$$\begin{aligned} N_{\text{cat}} &= C_{K0} \delta LA_c \\ \text{PCR} &= \frac{N_{\text{prod}}}{N_{\text{cat}}} = \frac{C_{A0} \sum \tilde{\Psi}_D \Delta \theta}{C_{K0} \delta}. \end{aligned}$$

In this study, the PCR was used to evaluate reactor performance and should not be mixed with the total turnover number (TTON) used to characterize the performance of a given catalyst (number of product molecules per catalyst site). The PCR values presented in this study were normalized in such a way that 100% conversion of the reactant in a batch reactor run would correspond to PCR = 100.

### Some Thoughts on Feasibility

In homogeneous catalysis large numbers of intermediate metal-organic complexes are normally generated during the reaction. This also would apply in the case of an immobilized

catalyst, which may well generate intermediates both in the stationary and in the flowing phase (Sheldon et al., 1998). This raises the question of whether reverse-flow operation would be unfeasible simply due to some of those intermediates not being adsorbed by the stationary phase. In this way, in some cases, those intermediates exit straight out with the flow and the catalysis cycle would be impaired.

However, from detailed studies of the reaction mechanisms and the kinetics of homogenous catalytic systems (see, for example, Garland and Feng, 1999) we can learn that the intermediate complexes usually form an equilibrium system. Similar to the case discussed in the paragraph on more complicated catalyst cycles, this would mean that the chromatographic retardation effect on the catalyst zone would occur even if only one of the intermediates in this equilibrium system were sufficiently adsorbed. All the reaction equilibria in this case would be shifted so that this adsorbed species would become the dominate intermediate.

This means that as long as the stationary phase generates all necessary intermediate complexes for enabling the catalytic cycle in the equilibrium system, and at least one of them is sufficiently adsorbed, reverse-flow operation could be feasible. That all necessary intermediates actually could be generated is proven by the existence of real functioning catalyst immobilizations (Sheldon et al., 1998).

The feasibility of reverse-flow operation has been considered with this background in mind. It is possible that this operation will be feasible in metal-organic catalysis if the system and the reaction are chosen judiciously (Garland, personal communication, 2001).

In the system studied by Hommeltoft et al. (1997), that is, the alkylation of isobutane with triflic acid catalyst, immobilized by absorption in a porous bed, the migration of the catalytic zone in the bed was studied. They could experimentally verify that this zone migrates slowed by a chromatographic effect due to the solubility in the flowing liquid phase of some intermediates in the catalysis cycle. This system has a complex catalytic chemistry, as in metal-organic catalysis. Thus their findings support that chromatographic migration also could occur in immobilized metal-organic systems, and consequently that reverse-flow operation could be a feasible way of compensating for catalyst leaching.

## Results and Discussion

### Simulation of the ideal case

At first, an ideal RFR was assumed to estimate the maximum performance. With an ideal RFR, we mean that the band broadening effect and the catalyst deactivation are neglected. The band broadening will be considered later. The simulations were carried out using Eqs. 4–8, with  $Pe$  and  $Da_2$  set to infinity.

An example of the concentration profile obtained on solving the model equations is presented in Figure 2. The flow direction is rightward, as shown. When the catalyst zone reaches the right end of the reactor, the sign of the flow is changed and the zone will move leftward. The small overshoots in concentrations shown in Figure 2 are numerical artifacts due to the use of an initial sudden step change in catalyst concentration. They have no significant effect on the calculated performance of the bed.

Either a homogeneous catalyst or a biphasic catalyst can be used in a batch reactor. The biphasic catalyst is often very expensive but advantageous, because the product can be separated easily from the catalyst after the reaction and the production can start again with the highest reaction rate by adding a new batch of reactant. If a homogeneous catalyst is used, recovery of the catalyst from the reaction mixture will be a major problem.

For the single-pass packed-bed reactor, the flow is unidirectional. The catalyst used in this reactor must be immobilized strongly onto the solid support without deactivation. However, a common problem for this kind of reactor is leakage of the catalyst from the solid support.

In Figure 3, the performance of the batch reactor, single-pass packed-bed reactor, and RFR are compared to PCR. Since the aim is to compare different types, the units on the axis will be arbitrary. The RFR is distinguished by the “piecewise-steady” curves because of the flow reversals. In all of the figures in the present article, the achieved conversion of all flow reactors is 77.5%. The conversion for the completely immobilized single-pass packed-bed reactor can be calculated by Eq. 14.

For the RFR, due to the movement of the catalyst zone, a longer space-time of the reactant in the catalyst zone should be taken into consideration.

Since the catalyst concentration is assumed to be 1% of the reactant, a PCR of 100 for the batch reactor here equals 100% conversion. In the beginning, the PCR increases faster for the batch reactor. But for the RFR, the PCR does not

increase until the reactor space-time is reached, which is after about 0.5 h. For example, an RFR needs 1.5 h to reach  $PCR = 77.5$ , while the batch reactor needs only 1 h.

However, the batch reactor using a homogeneous catalyst without separation of the catalyst and the reaction mixture has an upper limit of  $PCR = 100$  (when the proportion of 1% catalyst is used), which matches the fact that all reactant is converted.

This is when the advantage of the RFR comes in. The intersection of the curves of the RFR with that of the homogeneous batch reactor in Figure 3 shows how much more time an RFR needs to exceed the batch-reactor performance. The RFR can exceed this PCR limit and reach higher PCRs as long as the catalyst is kept within the RFR. In the long run, the production of the RFR will be higher. Just as with an ideal single-pass packed-bed reactor with no leakage, the RFR can reach an infinite PCR if band broadening and catalyst deactivation can be eliminated. However, we will see that the PCR reached is strongly limited by the band broadening.

The single-pass packed-bed reactor achieves a higher PCR than the RFR. However, for this to occur it is necessary that the catalyst be sorbed permanently onto the solid support and the activity on the solid support be as good as in the fluid phase. For many systems these conditions are not fulfilled because of catalyst leakage or activity reduction of the catalyst in the solid support.

If a *perfect* biphasic catalyst without leakage is available and the “replacement time” can be neglected, the batch reactor can reach the highest PCR. By “replacement time” we

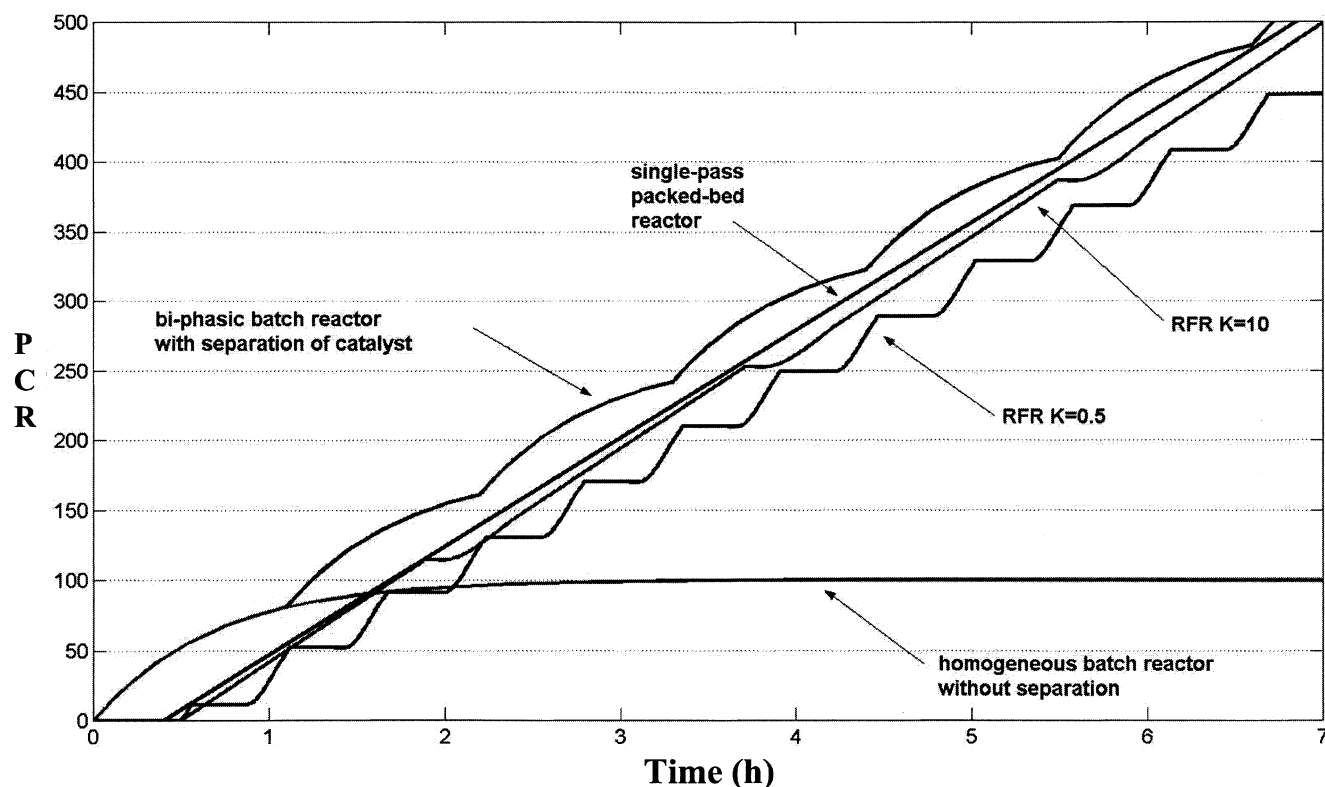


**Figure 3.** Comparison of performance between the batch reactor, completely immobilized single-pass packed-bed reactor, and RFR with two different  $K$  values,  $L = 4.5$  m,  $C_{K0} = 0.01$ ,  $\delta = 0.34$ ,  $Pe = \text{inf}$ ,  $Da_2 = \text{inf}$ .

The performance is expressed in PCR. The catalyst is active in both phases.

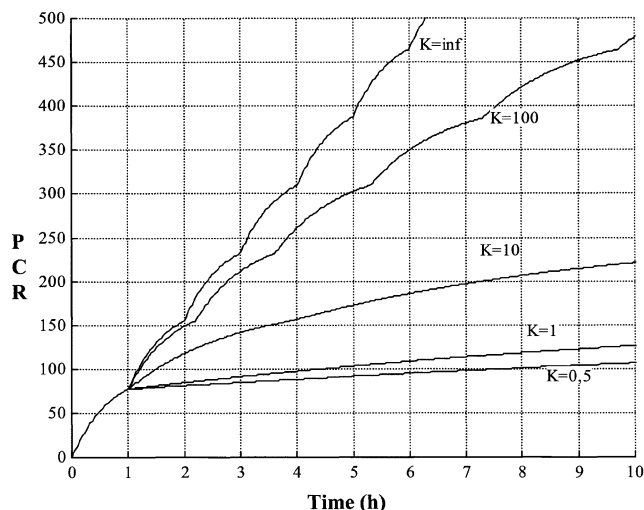


**Figure 4. Batch reactor with reuse of a leaking biphasic catalyst for different  $K$  values.**

Volume percent of catalyst is 5%.

mean the time it takes to separate the catalyst phase from the reaction mixture and reload a new batch of reactant. The biphasic batch reactor is superimposed on the homogeneous batch reactor in the first hour, after which it continues with the curved line.

Figure 4 shows the simulated performance of a batch reactor with a *leaking* biphasic catalyst that is reused. The same reactions and catalyst are assumed as for the RFR. Based on data for an immobilized catalyst system from the literature (Wöltinger et al., 1999), a catalyst volume percentage of 5% was used.

By comparing Figures 3 and 4 we can see that leaching will deactivate the biphasic catalyst more and more in each run. For  $K = 0.5$  this effect would be dramatic and for  $K = 10$  considerable, and the RFR would soon show higher PCRs than the batch reactor.

**Space Time.** Due to the movement of the catalyst zone, the first intuition would be that the length of an RFR has to be longer than a single-pass packed-bed reactor. However, if the steady-flow conversion (according to Eqs. 13 and 14) is constant in both cases, the fraction of the reactor length, consisting of the catalyst zone,  $\delta L$ , can actually be smaller, depending on the  $K$  value, resulting in the length of the RFR not necessarily having to be greater. This is due to the movement of the catalyst zone along with the reactant stream leading to a longer space time. It can be shown that in the ideal case without band broadening the amount of catalyst needed for a weakly adsorbed catalyst ( $K = 0.5$ ) is only half of that of a strongly adsorbed catalyst ( $K = 10$ ). However, a too low  $K$  value may lead to an insufficient separation of the product and the catalyst and, as shown below, the band-broadening effects are much worse at low  $K$  values.

**Case with no Activity on the Solid Support.** To see the impact of the performance when the catalyst is active only in the fluid phase, the RFR with  $K = 0.5$  is simulated again, but without component (C) participating in the first reaction. In this case, which is denoted case 2, an RFR with a high  $K$

value is not suitable, because the catalyst on the solid support is not active. Therefore, a low  $K$  value should be used.

Comparison of the two cases in Figure 5 shows that the decrease in performance is the factor

$$\frac{\epsilon}{\epsilon + K(1 - \epsilon)}, \quad (14)$$

which we can denote the activity reduction factor. To keep the same conversion as in case 1, the reactor length in case 2 has to be extended. Thus, more catalyst has to be used in case 2. Also, the RFR in case 2 needs almost 4 h to exceed the performance of a homogeneous batch reactor. We conclude that for a system with the catalyst active only in the fluid phase, a low  $K$  value is preferable. However, again band broadening may then become a serious problem.

### Band broadening

Until now we have assumed that the ideal case is one with no band-broadening effect. In reality, we expect that the band broadening or smearing of the catalyst zone together with catalyst deactivation are the factors that set the limit of the RFR performance. In our model, two mechanisms have been considered for band broadening. The first mechanism is kinetic resistance to sorption/desorption of the catalyst and the second is dispersion.

In this study, we estimate how long the flow reversal operation can last before it reaches a critical stop-parameter value. The stop parameter can be that the bandwidth exceeds a certain value or that the maximum concentration falls below a certain value. Here, the bandwidth has been defined as the part of the reactor length that has a concentration of  $B$  above 1% of  $C_{B0}$ . Flow reversal occurs when the catalyst zone reaches the end of the reactor and the simulation is stopped when the bandwidth reaches 90% of the reactor length. In reality, the “stop-parameter” can trigger a new catalyst feed, preferably in the midsection of the reactor, but here the “stop” ended the simulation. Also, due to band broadening, the time between the flow reversals will become shorter and shorter.

**Band Broadening Due to Kinetic Limitation.** The kinetic resistance means that the adsorption and desorption rates of the catalyst are finite. The  $Da_2$  number represents this rate, and until now  $Da_2$  has been infinite. To find out how the kinetic resistance affects the performance, calculations have been made for  $K = 0.5$  for different values of  $Da_2$ . Figure 6 shows the concentration profiles. In Figure 6a,  $Da_2$  is so large that the profiles of  $B$  and  $C$  are superimposed on each other, while the band broadening is considerable.

In Figures 6b and 6c, the PCR and the bandwidth increment are plotted. With  $Da_2 = 100$ , the band-broadening increment is so large that the PCR is greatly reduced and the catalyst almost smeared out in the reactor after 5 h, which triggered the “stop”. If  $Da_2$  becomes even lower, the curves of  $B$  and  $C$  will soon separate, as in chromatography, which means that the catalyst in the fluid phase ( $B$ ) will no longer be adsorbed onto the solid support. This peak separation will increase the bandwidth even further. With  $Da_2 = 1,000$ , the bandwidth increment is much lower, so that the PCR reached approaches the case with infinite  $Da_2$ . Thus a reactor system



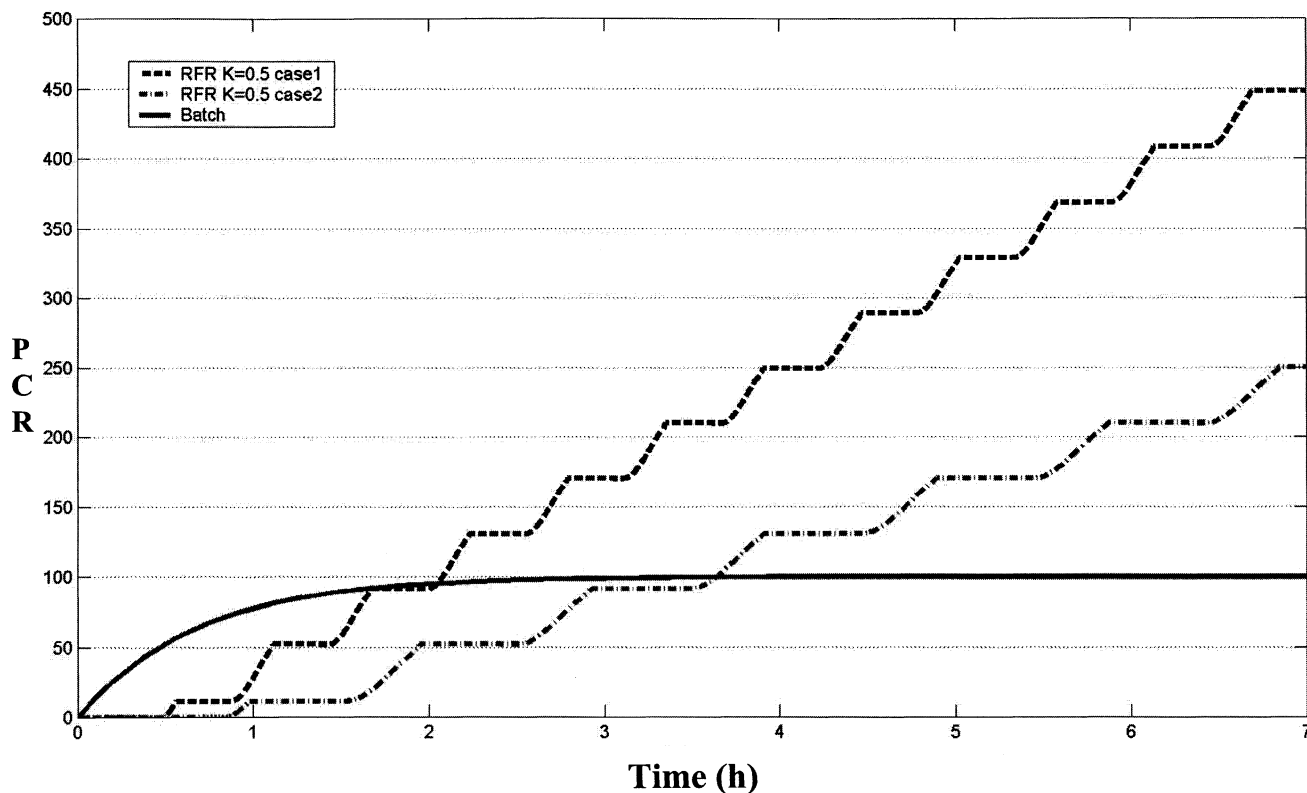


**Figure 5. Catalyst active in both phases (case 1) vs. catalyst active only in the fluid phase (case 2).**

The parameters for RFR case 1:  $L = 4.5$ ,  $\delta = 0.34$ , and for RFR case 2:  $L = 7.9$  m,  $\delta = 0.34$ . The  $K$  value is 0.5 and the steady-flow conversion is 77.5% for both cases.

with  $K = 0.5$  should strive for a  $Da_2$  higher than 1,000 (however, note that a lower  $Da_2$  value may be compensated for by using a longer reactor). Obviously, we will then get higher PCR than with the biphasic batch reactor, where even a second run with a catalyst with  $K = 0.5$  is questionable due to the high leakage (see Figure 4).

**Band Broadening Due to Dispersion.** The reactor Peclet number,  $Pe$ , represents the dispersion mechanism. The effect of dispersion is illustrated in Figure 7a. Figure 7 shows that  $Pe = 100$  for  $K = 0.5$  gives a significant impact on PCR and the bandwidth increment is unacceptably high. Observe that the high dispersion has led to flow reversal as the catalyst zone has reached the right end of the reactor. The “stop” for  $Pe = 100$  has occurred prior to 1 h, which can be seen in Figure 7b. As  $Pe$  increases to 500, the operation can last up to 5 h, but the PCR achieved is again too low. At  $Pe$  over 10,000, the PCR reached is close to the ideal case, and the effect of dispersion may be neglected. Note that with  $Pe$  a little higher than 1,000, the PCR from the RFR will become higher than for the biphasic batch reactor due to the high leakage of catalyst for  $K = 0.5$ .

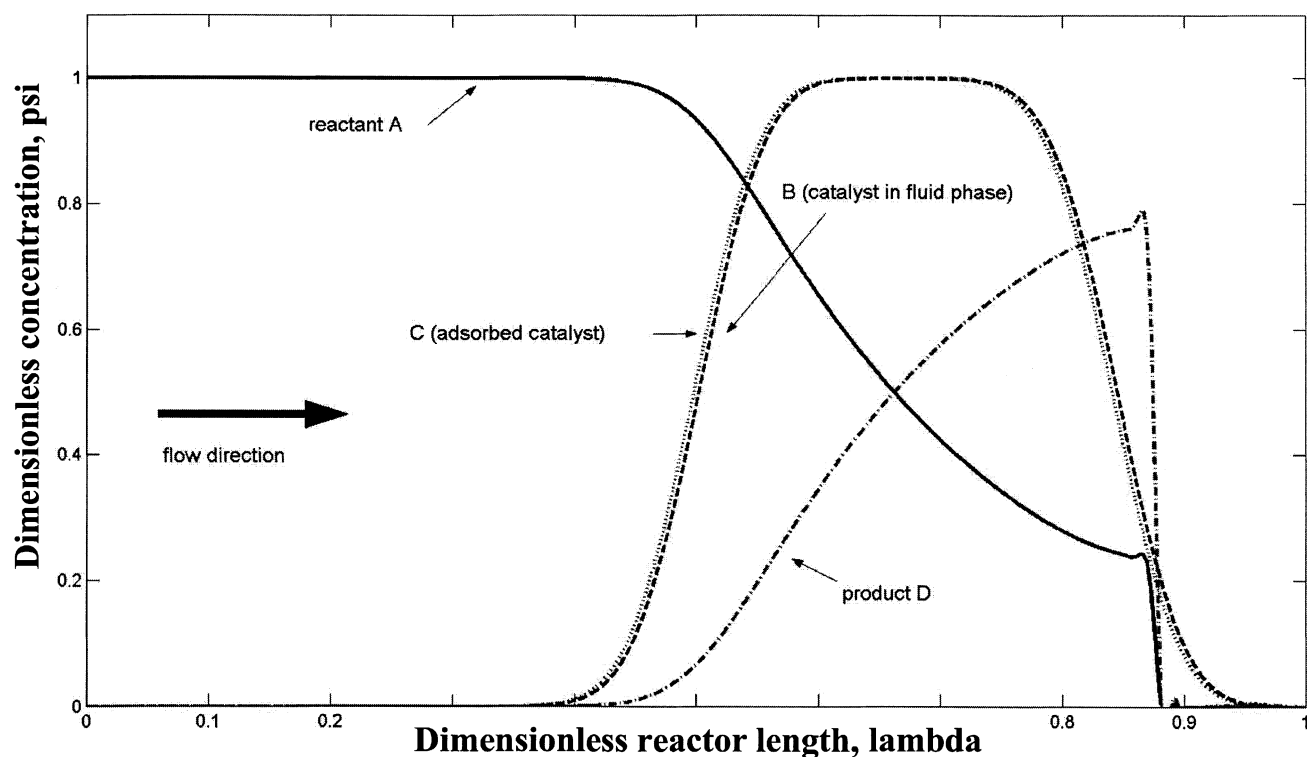
As can be seen in Figure 7c, the bandwidth increments are very high in the beginning because of the smearing of the square-shaped catalyst zone to a Gaussian peak. As time passes, the bandwidth increments decrease to a certain increment rate. The zigzag form of the curves for low  $Pe$  in Figure 7c is due to the boundary condition for the catalyst and is discussed below.

**Effect of the  $K$  Value.** In reality, there will always be a combination of dispersion and kinetic resistance effects that will reduce the operation time.

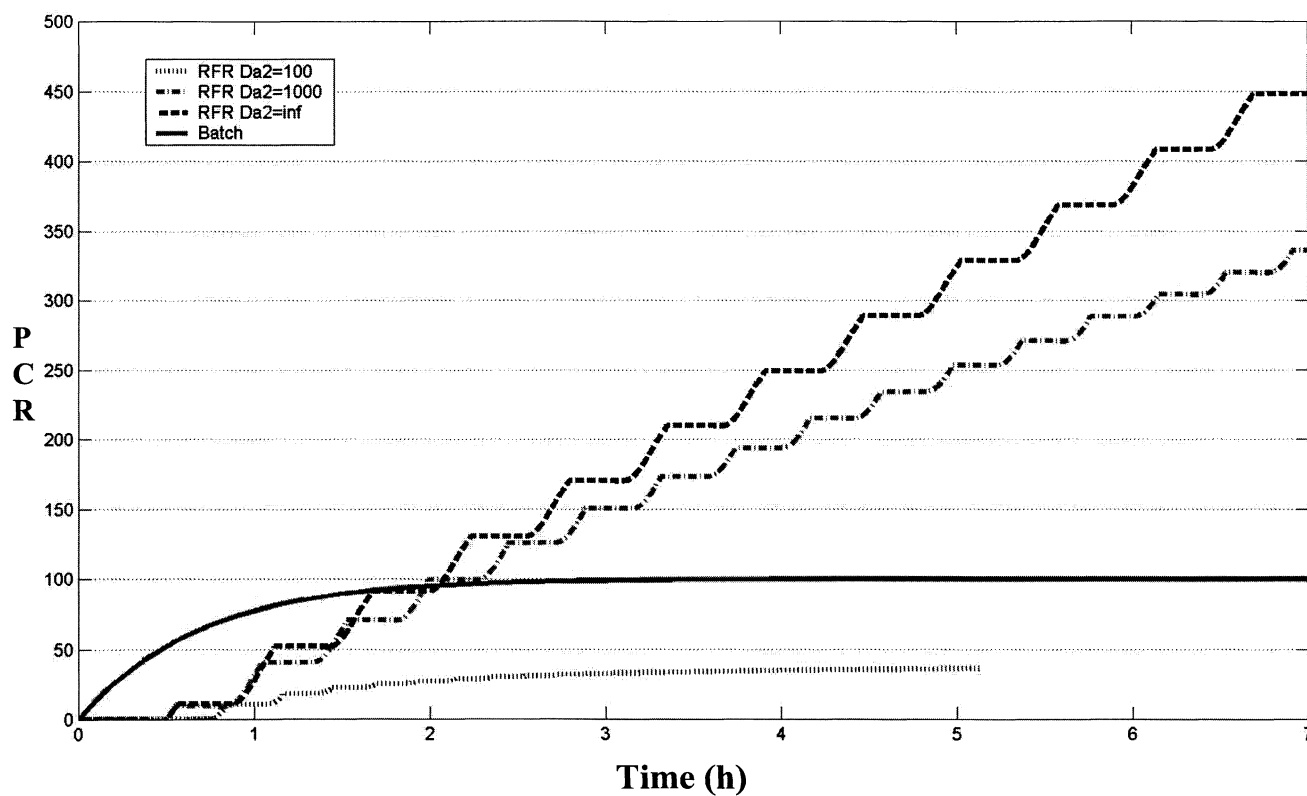
If the rate of band broadening is constant, that is,  $Pe$  and  $Da_2$  are constant, a higher  $K$  value may give a higher PCR in a shorter operation time period. This is due to fewer reversals compared to a lower  $K$  value. At the flow reversal, the efficiency is lowered. However, a lower  $K$  value will have the advantage of reaching a higher PCR in a longer time perspective, which is illustrated in Figure 8a. This is because a shorter catalyst zone is needed for a lower  $K$  value due to the longer space time. Therefore, it takes a longer time before the width of the catalyst zone exceeds the threshold value that triggers the stop mechanism, which can be seen in Figure 8b.

Note that by increasing the  $K$  value can obtain the same PCR with a lower Peclet number.

**Other Catalyst Concentrations.** So far, the maximum catalyst concentration  $C_{K0}$  has been set to 1% of the initial reactant concentration. However, if  $C_{K0}$  is increased, the length of the catalyst zone,  $\delta$ , can be made shorter so the total catalyst concentration in the reactor is kept constant. A shorter catalyst zone leads to a shorter space time in the zone (lower conversion), which is compensated for by a higher reaction rate in the zone due to a higher catalyst concentration (higher conversion). Also, a resulting effect is a longer operation time due to longer time between reversals. Figure 9 shows that a shorter catalyst zone is more advantageous. Thus, any system



(a)



(b)

**Figure 6. Band broadening due to finite values of  $Da_2$ .**

(a) Concentration profiles at  $\theta = 0.35$ , (b) PCR. Parameters for RFR:  $K = 0.5$ ,  $L = 4.5$  m,  $C_{K0} = 0.01$ ,  $\delta = 0.34$ ,  $Pe = \text{inf}$ , boundary conditions (BC) = case 1.

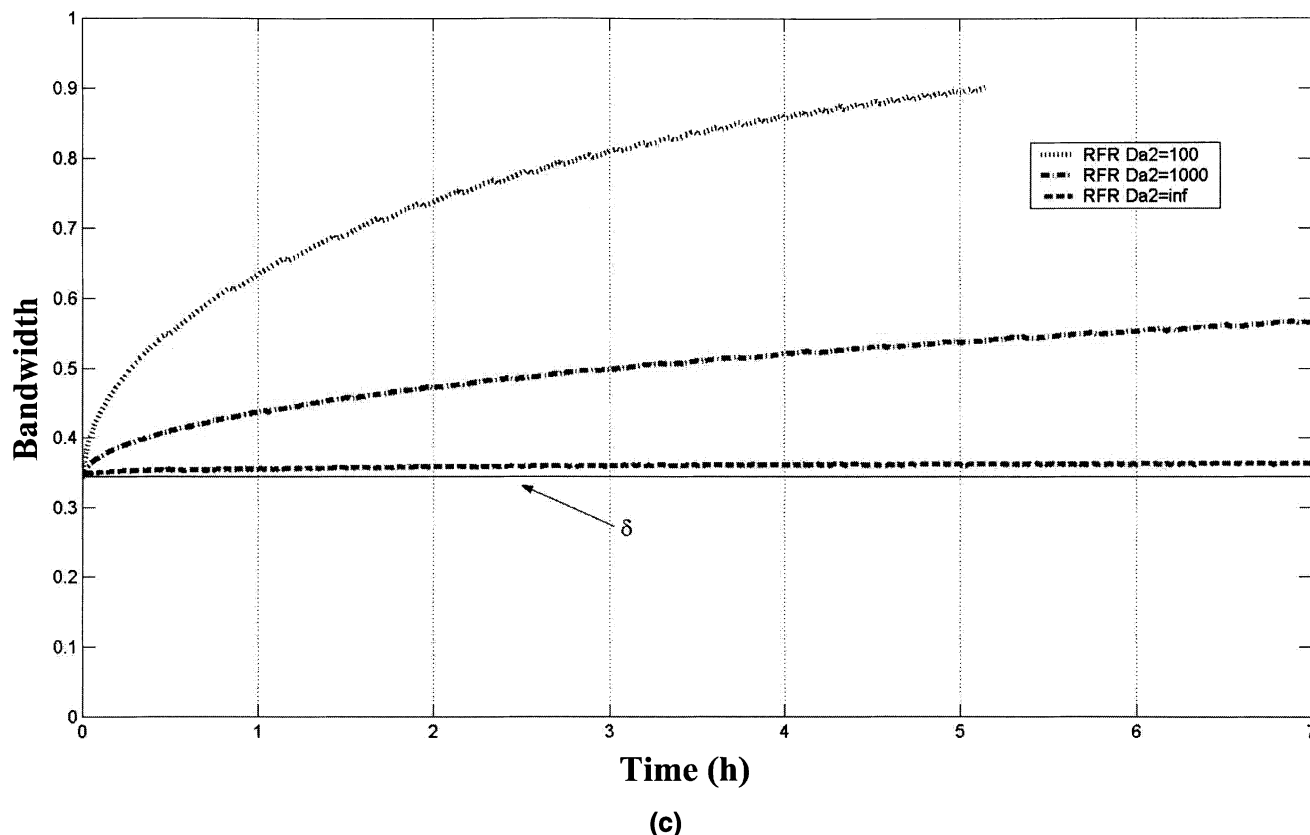


**Figure 6. Band broadening due to finite values of  $Da_2$ .**

(c) Bandwidth. Parameters for RFR:  $K = 0.5$ ,  $L = 4.5$  m,  $C_{K0} = 0.01$ ,  $\delta = 0.34$ ,  $Pe = \text{inf}$ , boundary conditions (BC) = case 1.

should have the shortest possible catalyst zone with a maximum concentration of catalyst, as long as no overloading occurs.

**Effect of Boundary Conditions and Bed Length.** All the results presented so far were calculated with boundary conditions as per case 1. A comparison of the two sets of boundary conditions revealed that the differences in the rate of change of the PCR could be safely neglected between the two cases. On the other hand, case 1 has less band broadening and significantly longer operation times than case 2 when Danckwerts boundary conditions are used for all differential equations; see Figure 10. The reason for this is that in case 1 there is considerable diffusion of catalyst out of the system when the catalyst zone is close to the outlet. The explanation of this is that this boundary condition causes a high concentration gradient immediately before and after flow reversal. This results in a decrease in the bandwidth as defined in this work. In case 2 the corresponding leakage is one order of magnitude less.

Due to the effect of the boundary conditions, the bandwidth and operation time are difficult to predict in a real system, since the boundary conditions are not easy to determine exactly. Our case 1 and case 2 are extremes, and real conditions are probably somewhere between. On the other hand, the bandwidth and operation time can be easily adjusted by changing the bed length.

Figure 11 illustrates the effect of bed length on bandwidth and operation time. The calculations assume that the length

of a bed is increased with a constant particle size, that is, the Peclet number based on the bed length increases correspondingly. Obviously, operation times can easily be increased considerably by fairly modest increases of the bed length.

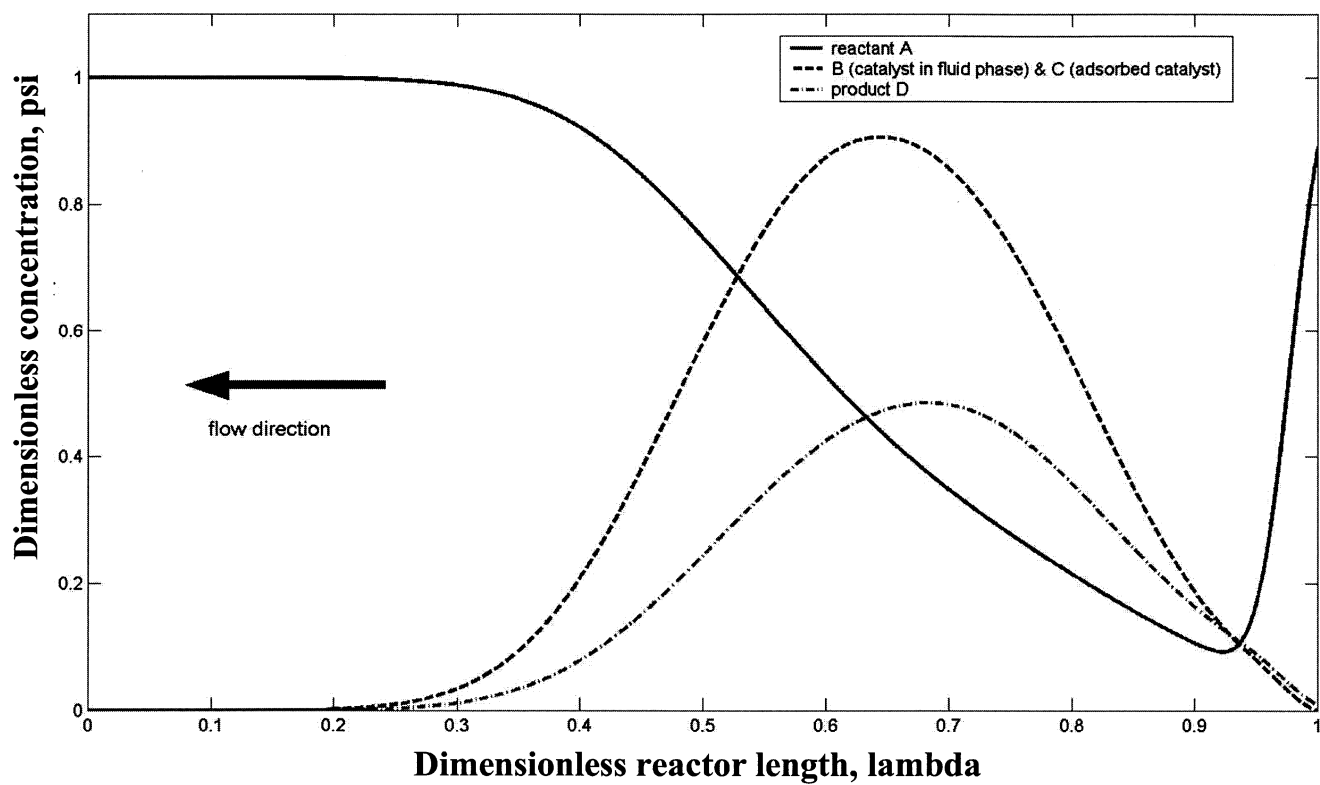
## Some Thoughts on Design and Operation

### *Quasi-continuous operation*

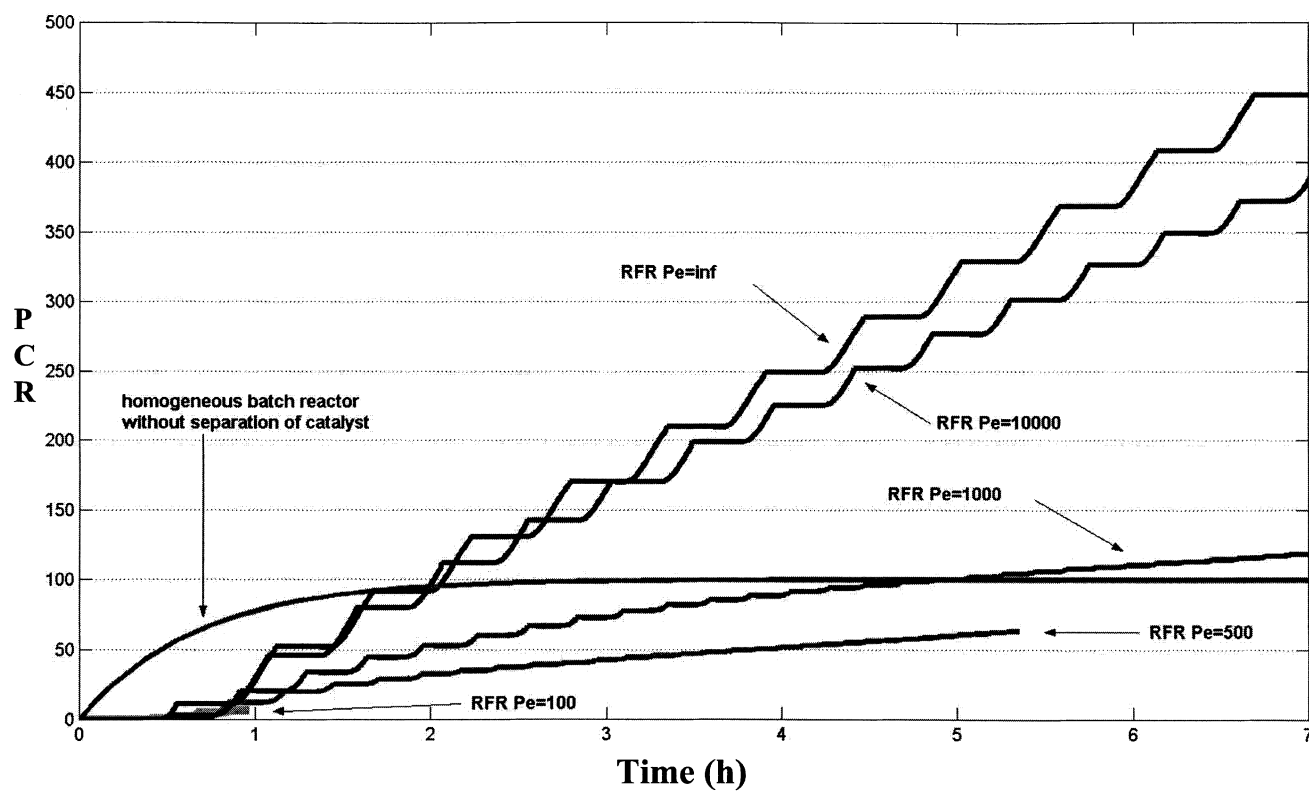
The RFR shown in Figure 1 is similar in design to the RFRs for heat and reactant mass trapping. Those reactors are continuous. However, the RFR in Figure 1 only can be operated continuously in the ideal case without band-broadening effects. With such effects present the catalyst zone will gradually expand and finally fill up the whole bed, so that further flow reversals are not possible. Then the operation must be stopped and the catalyst must be restored before continuing. Therefore, this mode of operation is called quasi-continuous.

### *Batchwise operation*

So far, we have implied that the RFR studied is a separate flow reactor. However, note that the catalytic packed bed may instead be part of a batch-reactor system with a tank and a recirculation loop. The catalytic packed bed would be placed in the recirculation loop; see Figure 12. In such a system the reverse-flow operation would simply mean that the recirculation flow is reversed periodically or when starting a new batch run.



(a)



(b)

**Figure 7. Band broadening due to dispersion mechanism  $Pe$ .**

(a) Concentration profiles at  $\theta = 0.4$ , (b) PCR. Parameters for RFR:  $K = 0.5$ ,  $L = 4.5$  m,  $C_{K0} = 0.01$ ,  $\delta = 0.34$ ,  $Da_2 = \text{inf}$ , (BC) = case 1.

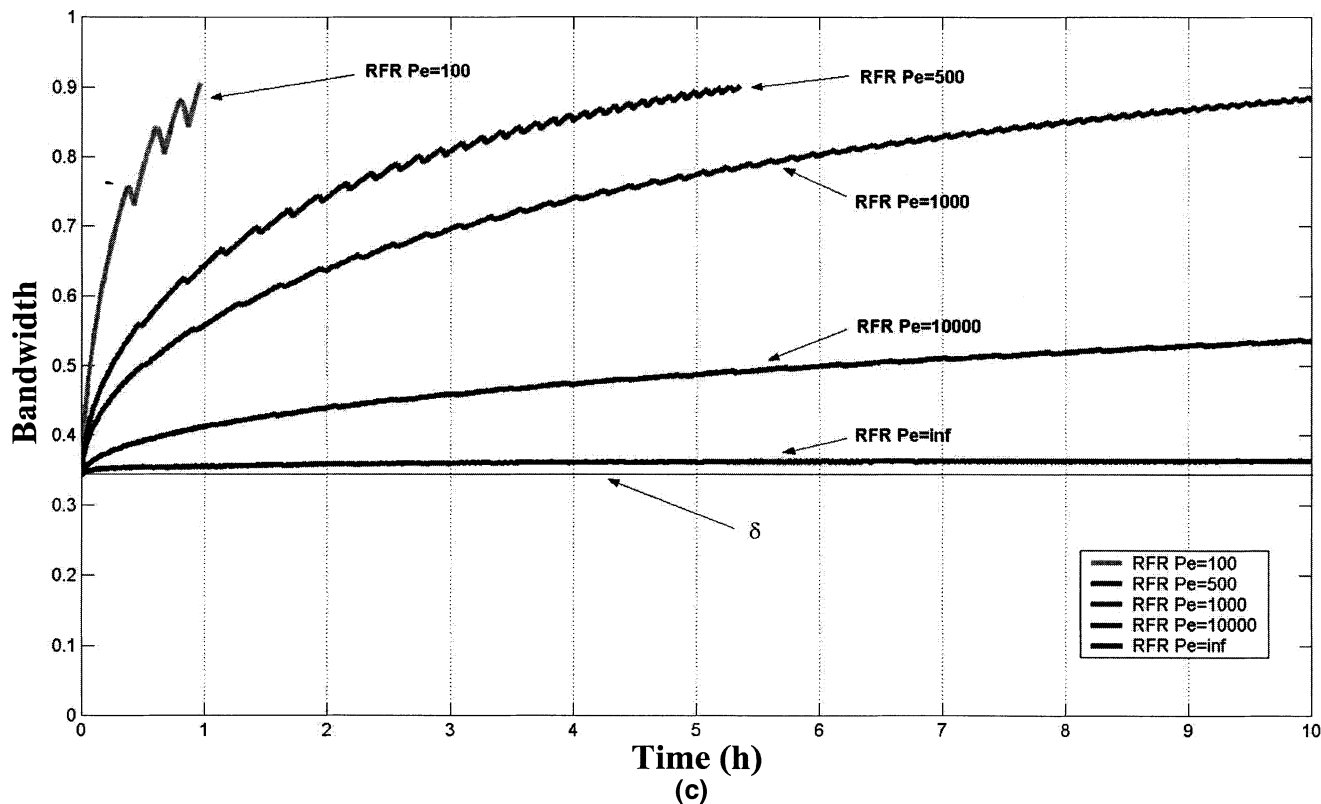


**Figure 7. Band broadening due to dispersion mechanism  $Pe$ .**

(c) Bandwidth. Parameters for RFR:  $K = 0.5$ ,  $L = 4.5$  m,  $C_{K0} = 0.01$ ,  $\delta = 0.34$ ,  $Da_2 = \text{inf}$ ,  $BC = \text{case 1}$ .

In this mode of operation, instead of adding the immobilized particulate catalyst as a slurry to the batch reactor, we are placing it as a packed bed in a recirculation loop of such a reactor. Note that in conventional operation using slurry the catalyst would be partially deactivated by leaching after each batch run, resulting in a practical limit on the number of runs. No such deactivation would occur in the packed bed operating with reverse flow, and in an ideal case without band broadening we would have no limit on the number of runs as far as deactivation by leaching is concerned.

However, a practical limit on the number of runs would result from the unavoidable band-broadening effects. Yet, with a proper bed design we can expect more batch runs from reverse-flow operation than from conventional operation with the catalyst used as slurry.

Finally this mode of operation has the advantage that most of the active catalytic substance will remain at a high concentration in the spent bed material. This should facilitate recovery of valuable catalyst substances. On the other hand, in slurry operation, most of the active catalyst substance will leave the system as a dilute solution in the mother liquor.

### Bed design

The choice of the best combination of mobile phase, solid support, and packing material will depend on several factors. For example, if the activation of the catalyst is reduced upon adsorption onto the solid support, a system with a low  $K$  value is more desirable. Catalyst deactivation and band broadening

limits the RFR. Here, the catalyst deactivation has been ignored, except by leaching. The band-broadening effect due to dispersion and mass transfer can reduce the performance considerably. With the reactor length  $K$  value studied in this work, and  $K = 10$ , this will happen if  $Pe < 1,000$  or  $Da_2 < 1,000$ , but for  $Pe > 100$  and  $Da_2 > 100$  performance is still rather good; see Figure 13. Therefore, it is of primary importance to first determine the band-broadening parameters. For example,  $Pe = 100$  would roughly correspond to the reactor length of 2 m if the particle size is 5 mm [see, for example, Levenspiel (1972)].  $Da_2 = 100$  for such a reactor and  $U = 0.001$  m/s gives a  $k_2a$  value of  $0.05 \text{ s}^{-1}$ , that is, the sorption/desorption equilibrium would have to be closely approached within a minute. The latter condition possibly appears somewhat more restrictive, but one should keep in mind that both increasing the reactor length and using systems with higher  $K$  values could relieve this restriction. Note that at  $K = 10$ , the catalyst immobilization is probably leaking too much for being reused in the slurry operation in a batch reactor; see Figure 4. Since  $k_2a$  represents an apparent rate coefficient that includes both external and internal mass transfer, decreasing particle size may also give an improved performance. However, due to the form of the Ergun pressure-drop equation, this would lead to a rapid increase in the pressure drop, which would soon be detrimental. However, the pressure drop over such a bed with 0.5-mm particles would still be less than 10 kPa for most fluids.

If the limitations can be diminished, the RFR may be a solution for homogeneous/heterogeneous catalysis in cases

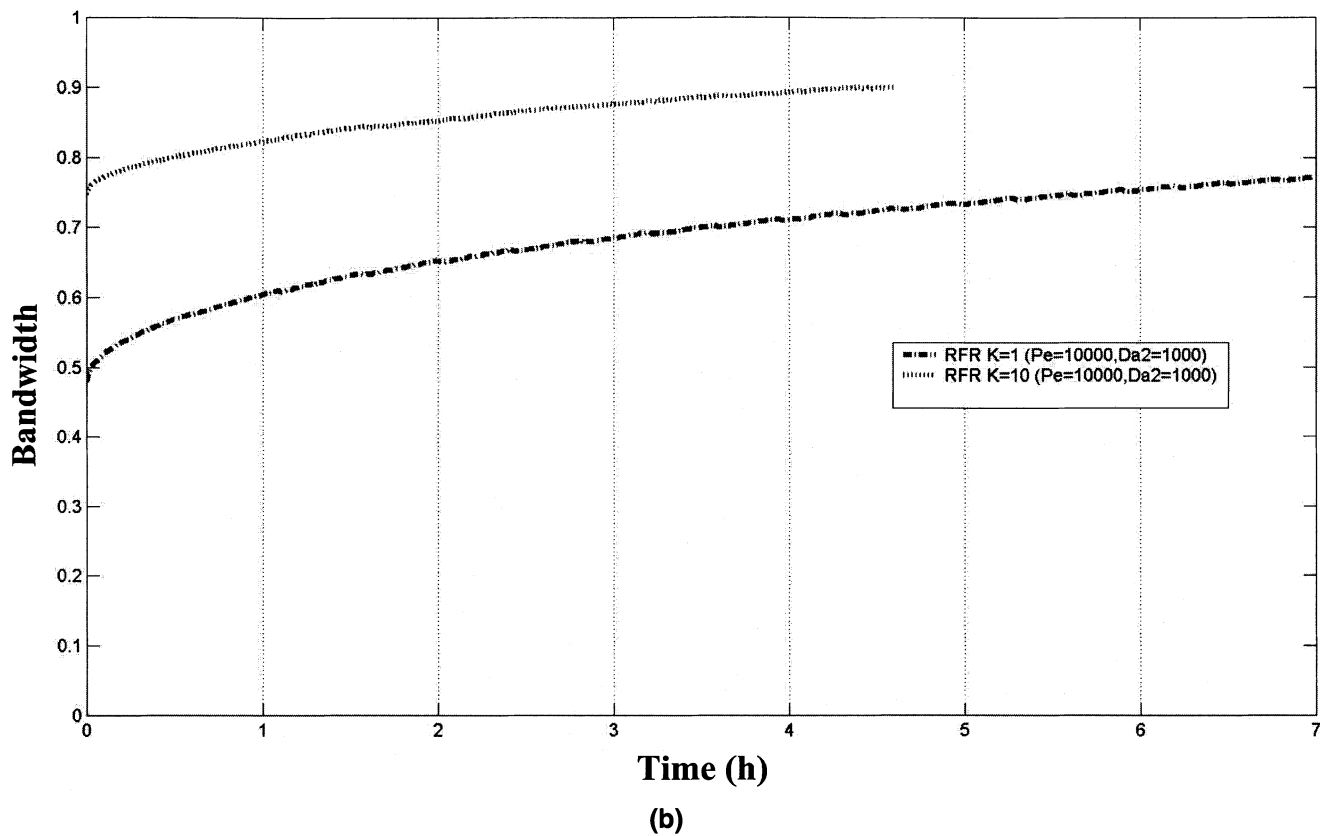
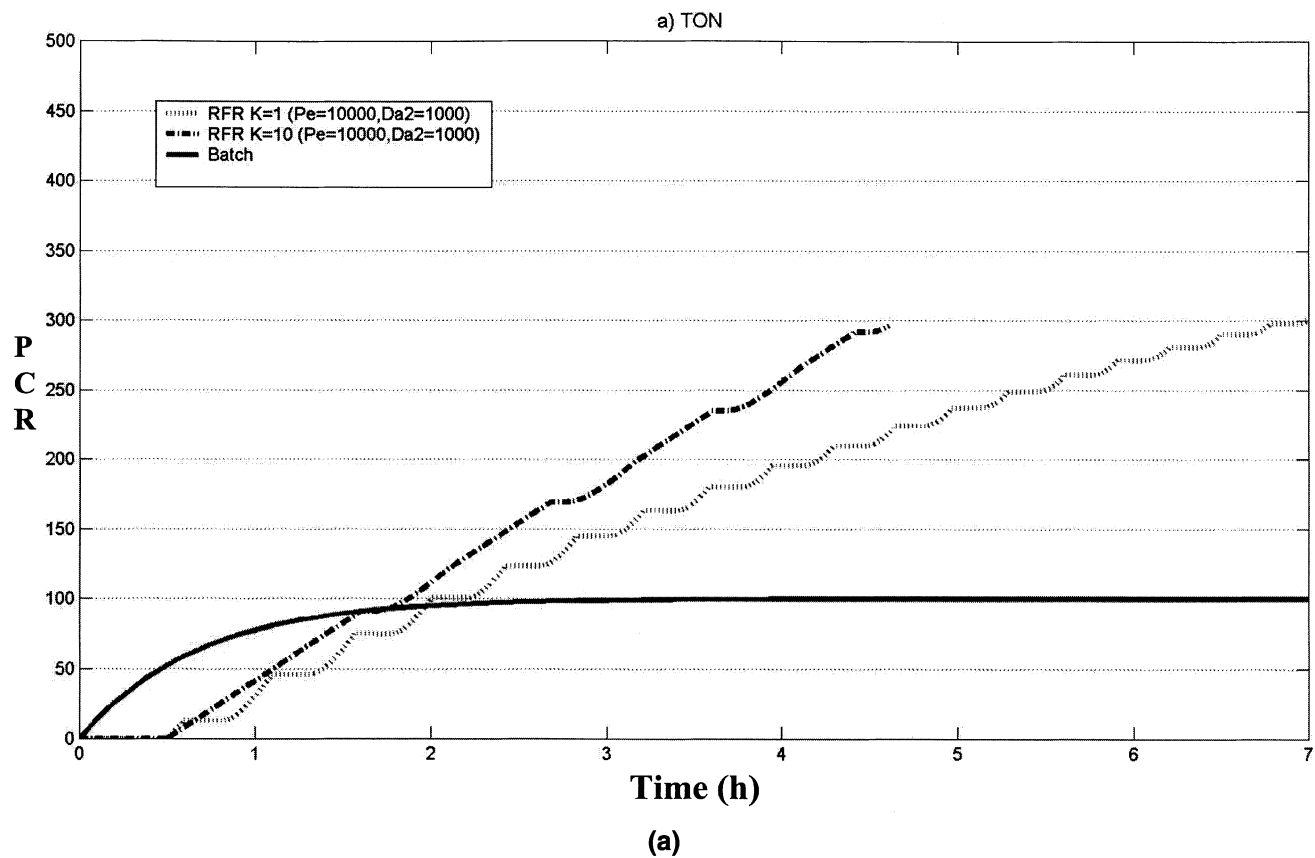


**Figure 8. Importance of  $K$  value.**

(a) PCR, (b) bandwidth. Parameters for RFR:  $Pe = 10,000$ ,  $Da_2 = 1,000$ ,  $L = 4.5$  m,  $C_{K0} = 0.01$ , BC = case 1.

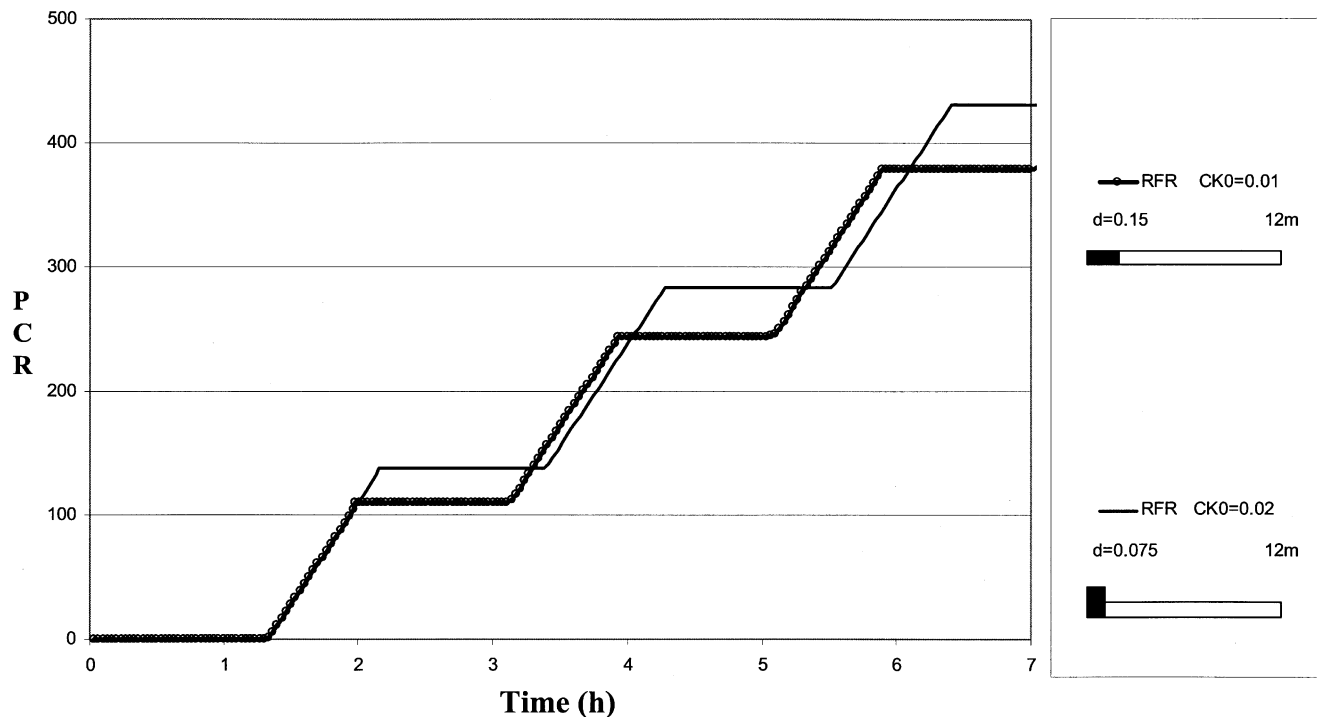


**Figure 9. Effect of shorter catalyst zone but higher concentration.**

The bold line represents an RFR with  $\delta = 0.15$  and  $C_{K0} = 1\%$ . The thin line represents an RFR with shorter zone  $\delta = 0.075$  and  $C_{K0} = 2\%$ . BC = case 1. The height of the filled parts represents the catalyst concentration in the zone,  $C_{K0}$ .

where catalyst recovery in the batch system is inefficient and no perfectly leakage-free immobilization is possible. We have shown several cases in our simulations where the RFR with band broadening performs better in terms of PCR than the corresponding biphasic batch reactor with catalyst reuse.

### Potential application

Currently, it is not possible to give an example of a system that we know will function in reality. However, we have chosen, by a simple discussion, to explore the possibilities of one kind of catalyst system for oxidation with air or hydrogen per-

oxide recently described in the literature, that is, cobalt macrocycles immobilized by means of encapsulation in zeolite particles (Wöltinger et al., 1999). These authors have tested an immobilized cobalt macrocycle catalyst by batch experiments, reusing the catalyst three times. The pattern of increasing residence times between the runs needed to obtain the desired conversion resembles the pattern shown in Figure 4, suggesting a significant leaching tendency (this could, of course, be some other type of catalyst deactivation, but we assume leaching here). We do not know whether this

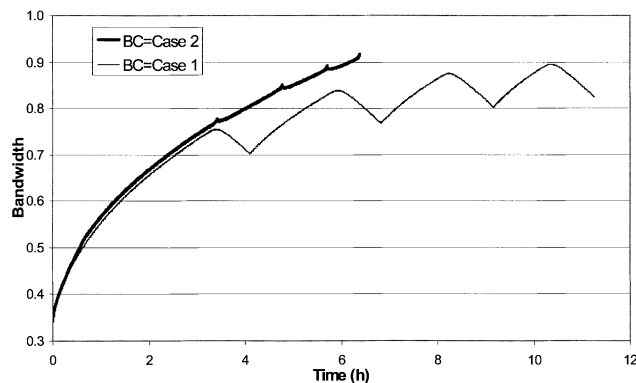


**Figure 10. Effect of boundary conditions on bandwidth and operation time.**

$K = 10$ ,  $Pe = 100$ ,  $Da_2 = \text{inf}$ ,  $L = 4.5$  m.

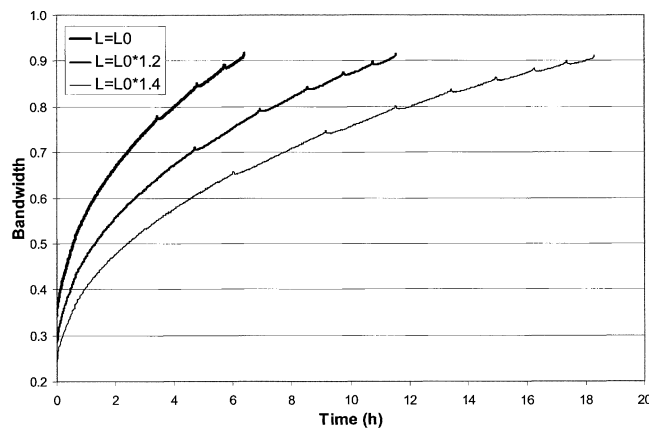


**Figure 11. Effect of bed length on bandwidth and operation time.**

$K = 10$ ,  $Pe = 100$ ,  $Da_2 = \text{inf}$ ,  $L_0 = 4.5$  m, BC = case 2.  $\delta L = 0.34 * L_0$  in all three cases.

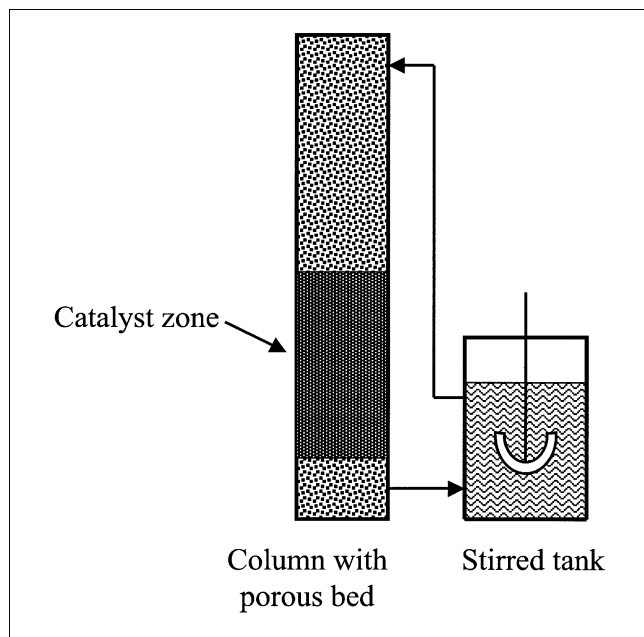


**Figure 12. Batchwise operation of an immobilized catalyst in a porous bed with reverse-flow operation.**

When the catalyst zone reaches the lower end of the bed, the flow is reversed.

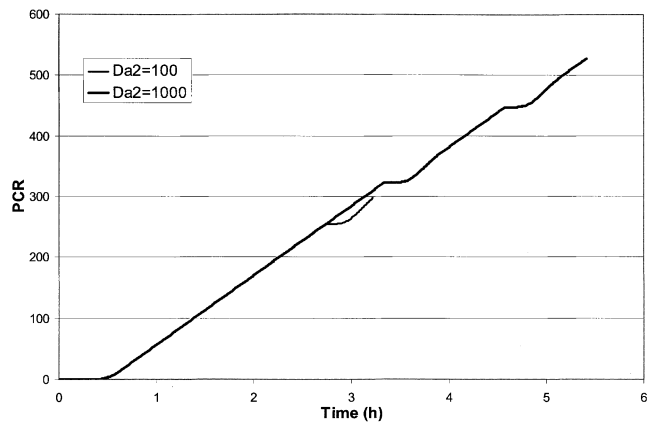
leaching is reversible or not, but an irreversible leaching process would probably show a different pattern for the increase in the residence times between runs.

A possible application could be an oxidation reaction with hydrogen peroxide as the oxidant. Hydrogen peroxide would act on the cobalt macrocycle residing in a zeolite bed mounted in a recirculation loop over the batch reactor tank. In turn, the cobalt macrocycle would act on a series of other catalytic species in the solution that in turn act on the reactant to be oxidized [the details can be found in Wöltinger et al. (1999)]. Reverse-flow operation would occur simply by reversing the recirculating flow, aiming to keep the cobalt macrocycle within the zeolite bed. Note that with such a system we need not necessarily work with a high conversion over the packed bed. Therefore, we can take advantage of using smaller particles, compensating for increased pressure drop by using a shorter bed length.

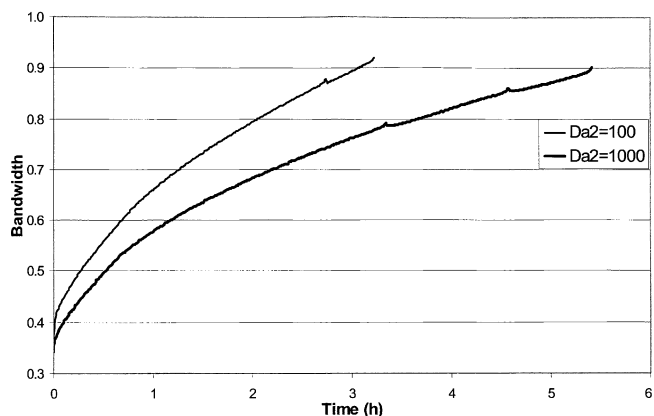
## Conclusions

For ideal systems with no band-broadening effects and catalyst deactivation, except by leaching, unlimited reverse flow operation may be possible for a leaking immobilized catalyst. This would be an important advantage compared to reusing the same catalyst in the form of slurry in batch-reactor operation, burdened by the accumulating loss of catalyst by leaching.

The key issue in such cases is whether the leakage process is reversible or irreversible. Only systems with reversible leakage, resulting in a chromatographic catalyst migration in the packed bed, are feasible for reverse flow operation.



(a)



(b)

**Figure 13. (a) PCR; (b) bandwidth for  $K = 10$ ,  $Pe = 100$ ,  $BC = \text{case 2}$ .**

For ideal systems with two or more complexes in the catalytic cycle a separation effect may occur, disabling the catalytic reaction at the ends of the catalyst zone. However, this effect is reversible and may not prevent unlimited reverse-flow operation.

Compared to a PFR with perfectly immobilized catalyst, the ideal RFR may well require less catalyst for the same conversion. This is due to prolonged contact between catalyst and reactant as a result of the catalyst migration in the bed.

In reality, band-broadening effects occur by kinetic and dispersion effects and will result in an upper limit for the number of flow reversals.

The results of the numerical simulations of a simple system suggest that even with band broadening, it may be possible to obtain significant advantages compared to batch operation with catalyst reuse. For every combination of the Peclet and the Damköhler numbers, characterizing the band-broadening effect, there is a certain number of possible flow reversals. This number can be increased as much as desired by simply increasing the bed length.

As an overall conclusion, our theoretical study and numerical simulations suggest that it may be possible to significantly decrease the requirements of very strong bonds between cat-



alyst and support and low catalyst solubility by using a reverse-flow operation in a packed bed. Thus, this technique may enable the immobilization of homogeneous metal organic catalysts for which other immobilization methods have failed.

## Acknowledgments

The Swedish Foundation for Strategic Research (SSF) and KTH Holding AB have financially supported this work. It was a part of the SELCHEM-program (Selective Preparation of Fine Chemicals and Pharmaceuticals). We thank Gunnar Erlandsson, SELCHEM, and Kenneth Billquist, KTH Holding AB, for valuable discussions, and our colleague Christina Hörnell for her suggestions and helpful discussions.

## Notation

$a$  = surface area of interface per unit reactor volume,  $\text{m}^2/\text{m}^3$   
 $A_c$  = cross-sectional area of reactor,  $\text{m}^2/\text{m}^3$   
 $C_{K0}$  = total concentration of catalyst,  $\text{mol}/\text{m}^3$   
 $C_{x0}$  = initial concentration of component  $X$ ,  $\text{mol}/\text{m}^3$   
 $Da_1$  = Damköhler number for the reaction rate  
 $Da_2$  = Damköhler number for the adsorption/desorption rate  
 $D_e$  = effective dispersion coefficient in reactor,  $\text{m}^2/\text{s}$   
 $k_1$  = specific reaction rate,  $\text{m}^3/\text{mol} \cdot \text{s}$   
 $k_2$  = mass-transfer coefficient for the catalyst,  $\text{m}/\text{s}$   
 $K$  = equilibrium constant for the catalyst adsorption  
 $L$  = reactor length,  $\text{m}$   
 $Pe$  = reactor Peclet number  
 $T$  = time,  $\text{s}$   
 $PCR$  = normalized turnover number  
 $TOF$  = turnover frequency,  $\text{s}^{-1}$   
 $U$  = superficial velocity,  $\text{m}/\text{s}$   
 $X$  = steady-state conversion over the catalyst zone

## Greek letters

$\delta$  = fraction of reactor consisting of catalyst zone initially  
 $\epsilon$  = bed porosity  
 $\lambda$  = dimensionless distance from reactor inlet  
 $\Psi_x$  = dimensionless concentration of component  $X$   
 $\theta$  = dimensionless time

## Subscripts

$f$  = fluid phase  
 $s$  = solid support

## Literature Cited

- Agar, D. W., and W. Ruppel, "Multifunktionale Reaktoren für die Heterogene Katalyse," *Chem. Ing. Tech.*, **60**, 731 (1988).  
 Blanks, R. F., T. S. Wittrig, and D. A. Peterson, "Bidirectional Adiabatic Synthesis Gas Reactor," *Chem. Eng. Sci.*, **45**, 2407 (1990).  
 Björnbo, P., K. G. W. Hung, M. Anderlund, and B. Åkermark, "Reverse Flow Operation for Catalyst Trapping," AIChE Meeting, Reno, NV (2001).  
 Björnbo, P., and B. Åkermark, "A Catalytic Process in a Flow Reversal Reactor," PCT Patent Application WO 01/28674, to KTH Holding AB (April 26, 2001).  
 Bobrova, L. N., E. M. Slavinskaya, A. S. Noskov, and Yu. Sh. Matros, "Unsteady-State Performance of  $\text{NO}_x$  Catalytic Reduction by  $\text{NH}_3$ ," *React. Kinet. Catal. Lett.*, **37**, 267 (1988).  
 Boreskov, G. K., Yu. Sh. Matros, and O. V. Kiselev, "Catalytic Processes Carried out Under Nonstationary Conditions: Thermal Front in a Fixed Bed of Catalyst," *Kinet. Catal.*, **20**, 773 (1979).

- Boreskov, G. K., and Yu. Sh. Matros, "Unsteady-State Performance of Heterogeneous Catalytic Reactions," *Catal. Rev.-Sci. Eng.*, **25**, 551 (1983).  
 Cornil, S. B., and E. Kuntz, "Introducing TPPTS and Related Ligands for Industrial Biphasic Processes," *J. Organomet. Chem.*, **502**, 177 (1995).  
 Cottrell, F. G., "Purifying Gases and Apparatus Therefore," U.S. Patent No. 2,171,733 (June 21, 1938).  
 Falle, S. A. E. G., J. Kallrath, B. Brockmüller, A. Schreieck, J. R. Giddings, D. W. Agar, and O. Watzenberger, "The Dynamics of Reverse Flow Chromatographic Reactors with Side Stream Feed," *Chem. Eng. Commun.*, **135**, 185 (1995).  
 Femlab, *User's Guide and Introduction*, COMSOL AB, Stockholm (1999).  
 Garland, M., and J. Feng, "Unmodified Homogeneous Rhodium-Catalyzed Hydroformylation of Styrene. The Detailed Kinetics of the Regioselective Synthesis," *Organometallics*, **18**, 417 (1999).  
 Heck, R. F., "Palladium-Catalyzed Vinylation of Organic Halides," *Org. React.*, **27**, 345 (1982).  
 Hommeltoft, S. I., O. Ekelund, and J. Zavilla, "Role of Ester Intermediates in Isobutane Alkylation and Its Consequence for the Choice of Catalyst System," *Ind. Eng. Chem. Res.*, **36**, 3491 (1997).  
 Hommeltoft, S. I., and H. F. A. Topsoe, "Alkylation Process," European Patent Application EP 0 433 954 A1, to Haldor Topsoe A/S (June 26, 1991).  
 Hung, K. G. W., M. Anderlund, B. Åkermark, and P. Björnbo, "A Reverse Flow Reactor for Homogeneous/Heterogeneous Catalysis," AIChE Meeting, Los Angeles, CA (2000).  
 Kallrath, J., A. Schreieck, B. Brockmüller, D. W. Agar, O. Watzenberger, S. A. E. G. Falle, and J. R. Giddings, "Simulation of Chromatographic Reactors," *Comput. Chem. Eng.*, **18** (Suppl.), 331 (1993).  
 Khinast, J., Y. O. Jeong, and D. Luss, "Dependence of Cooled Reverse-Flow Reactor. Dynamics on Reactor Model," *AIChE J.*, **45**, 299 (1999).  
 Levenspiel, O., *Chemical Reaction Engineering*, 2nd ed., Wiley, New York, p. 282 (1972).  
 Matros, Yu. Sh., and G. A. Bunimovich, "Reverse-Flow Operation in Fixed Bed Catalytic Reactors," *Catal. Rev. Sci. Eng.*, **38**, 1 (1996).  
 Matros, Yu. Sh., G. A. Bunimovich, V. O. Strots, and E. A. Mirosh, "Reversed Flow Converter for Emission Control After Automotive Engines," *Chem. Eng. Sci.*, **54**, 2889 (1999).  
 Neophytides, S. G., and G. G. Froment, "A Bench Scale Study of Reversed Flow Methanol Synthesis," *Ind. Eng. Chem. Res.*, **31**, 1583 (1992).  
 Neophytides, S. G., and A. Tripakis, "The Transient Operation of a Solid Oxide Fuel Cell Monolith Under Forced Periodic Reversal of the Flow," *Can. J. Chem. Eng.*, **74**, 719 (1996).  
 Nieken, U., G. Kolios, and G. Eigenberger, "Fixed-Bed Reactors with Periodic Flow Reversal: Experimental Results for Catalytic Combustion," *Catal. Today*, **20**, 355 (1994).  
 Sheldon, R. A., M. Wallau, I. W. C. E. Arends, and U. Schuchardt, "Heterogeneous Catalysis for Liquid-Phase Oxidations: Philosophers' Stones or Trojan Horses?" *Acc. Chem. Res.*, **31**, 485 (1998).  
 Snyder, J. D., and B. Subramanian, "Numerical Simulation of a Reverse-Flow  $\text{NO}_x$ -SCR Reactor with Side-Stream Ammonia Addition," *Chem. Eng. Sci.*, **53**, 727 (1998).  
 van de Beld, B., *Air Purification by Catalytic Oxidation in a Adiabatic Packed-Bed Reactor with Periodic Flow Reactor*, PhD Thesis, Univ. of Twente, Enschede, The Netherlands (1995).  
 Wöltinger, J., J. E. Bäckvall, and A. Zsigmond, "Zeolite-Encapsulated Cobalt Salophen Complexes as Efficient Oxygen-Activating Catalysts in Palladium-Catalyzed Aerobic 1,4-oxidation of 1,3-dienes," *Chem. Eur. J.*, **5**, 1460 (1999).  
 Züfle, H., and T. Turek, "Catalytic Combustion in a Reactor with Periodic Flow Reversal: 1. Experimental Results," *Chem. Eng. Process.*, **36**, 327 (1997).

Manuscript received Dec. 4, 2001, and revision received June 27, 2002.